Cell Biol Toxicol (2016) 32:333–345
DOI 10.1007/s10565-016-9338-9

ORIGINAL ARTICLE

Caudatin induces caspase-dependent apoptosis in human glioma cells with involvement of mitochondrial dysfunction and reactive oxygen species generation

Liang-zhen Zhu · Ya-jun Hou · Ming Zhao · Ming-feng Yang · Xiao-ting Fu · Jing-yi Sun · Xiao-yan Fu · Lu-rong Shao · Hui-fang Zhang · Cun-dong Fan · Hong-li Gao · Bao-liang Sun

Received: 19 October 2015 / Accepted: 6 May 2016 / Published online: 16 May 2016

Abstract Caudatin as one species of C-21 steroidal from *Cynanchum bungei decne* displays potential anticancer activity. However, the underlying mechanisms remain elusive. In the present study, the growth suppressive effect and mechanism of caudatin on human glioma U251 and U87 cells were evaluated in vitro. The results indicated that caudatin significantly inhibited U251 and U87 cell growth in both a time- and dose-dependent manner. Flow cytometry analysis revealed that caudatin-induced cell growth inhibition was achieved by induction of cell apoptosis, as convinced by the increase of Sub-G1 peak, PARP cleavage and activation of caspase-3, caspase-7 and caspase-9. Caudatin treatment also resulted in mitochondrial dysfunction which correlated with an imbalance of Bcl-2 family members. Further investigation revealed that caudatin triggered U251 cell apoptosis by inducing reactive oxygen species (ROS) generation through disturbing the redox homeostasis. Moreover, pretreatment of caspase inhibitors apparently weakens caudatin-induced cell killing, PARP cleavage and caspase activation and eventually reverses caudatin-mediated apoptosis. Importantly, caudatin significantly inhibited U251 tumour xenografts in vivo through induction of cell apoptosis involving the inhibition of cell proliferation and angiogenesis, which further validate its value in combating human glioma in vivo. Taken together, the results described above all suggest that caudatin inhibited human glioma cell growth by induction of caspase-dependent apoptosis with involvement of mitochondrial dysfunction and ROS generation.

Keywords Caudatin · Glioma · Apoptosis · Caspase · Bcl-2 family · Reactive oxygen species

Liang-zhen Zhu, Ya-jun Hou and Ming Zhao contributed equally to this work.

Electronic supplementary material The online version of this article (doi:10.1007/s10565-016-9338-9) contains supplementary material, which is available to authorized users.

L.-z. Zhu · B.-l. Sun (✉)
Affiliated Hospital of Taishan Medical University, Taian, Shandong 271000, China
e-mail: blsun88@163.com

Y.-j. Hou · M.-f. Yang · X.-t. Fu · J.-y. Sun · X.-y. Fu · L.-r. Shao · H.-f. Zhang · C.-d. Fan (✉) · B.-l. Sun
Key Lab of Cerebral Microcirculation in Universities of Shandong, Taishan Medical University, Taian, Shandong 271000, China
e-mail: tcdfan66@163.com

M. Zhao
Departments of Orthopaedics, Taian Central Hospital, Taian, Shandong 271000, China

H.-l. Gao (✉)
School of Pharmacy, Taishan Medical University, Taian, Shandong 271000, China
e-mail: ghl007@163.com

Introduction

Glioma is one of the most common malignant tumours of the nervous system, which has high mortality and

morbidity (Tseng and Tseng 2005). Due to its high infiltration and invasion capacity into adjacent tissues, the traditional therapies, such as the surgery, radiotherapy, chemotherapy or combined treatments, still cannot achieve the desired therapeutic effect (Adair et al. 2014; Demuth et al. 2008; Wang et al. 2015a, b; Zhang et al. 2014; Teschke and Eickhoff 2015). Hence, novel chemotherapeutic drugs with high efficacy and low toxicity are urgently needed to combat human glioma in clinical practice.

Recently, traditional Chinese medicines (TCMs) attract more attention in treatment of human tumours, improvement of life quality, prevention of recurrence and metastasis and reducing the complications of tumour chemotherapy (Wang et al. 2015a, b). *Cynanchum auriculatum* (*C. auriculatum*) as a TCM has been reported to nourish the blood and enhance immunity (Ma et al. 2011; Peng and Ding 2015). C-21 steroidal glycosides belong to the *Asclepiadaceae* family that exhibit potential ability in inhibiting cancer cells proliferation and invasion by induction of cell apoptosis (Li et al. 2014; Wang et al. 2011, 2013). Caudatin, a species of C-21 steroidal isolated from the root of *Cynanchum bungei decne* in China, displays multiple pharmacological functions, such as anticancer, immune regulation, hepatoprotection, antiaging, antioxidation, antiviral and neuroprotection (Luo et al. 2013; Zhang et al. 2007; Peng et al. 2008; Lv et al. 2009). The chemical structure of caudatin can be found in our previous publication (Fu et al. 2015). It is reported that caudatin could induce cell apoptosis in several types of cancer cell lines (Wang et al. 2015a, b). For instance, Fei et al. reported that caudatin could induce caspase-dependent apoptosis in HepG2 human hepatocarcinoma with involvement of Bcl-2 family change and activation of ERK and JNK (Fei et al. 2012). We previously explored that caudatin inhibited human glioma cell growth by induction of cell cycle arrest in 48 h (Fu et al. 2015). However, the underlying mechanism of caudatin-induced apoptosis remains unclear, especially the molecular mechanism in human brain tumours.

In the present study, we evaluated the anticancer activities and molecular mechanism of caudatin on human glioma cells, and the results showed that caudatin effectively inhibited human glioma cell growth in vitro by induction of caspase-dependent apoptosis with involvement of mitochondrial dysfunction and reactive oxygen species (ROS) generation. Moreover, caudatin significantly inhibited U251 tumour xenografts in vivo through induction of cell apoptosis involving the inhibition of cell proliferation and angiogenesis, which validated the therapeutic potency in clinic.

Materials and methods

Chemical

Caudatin (dissolved with 100 % dimethyl sulfoxide), propidium iodide (PI), JC-1 and MTT [3-(4, 5-dimethylthiazol-2-yl)-2, 5-diphenyltetrazolium bromide], glutathione (GSH) and other reagents were all purchased from Sigma. DCFH-DA, mitoSOX and BCA assay kit was bought from Beyotime Institute of Biotechnology. Dulbecco's modified Eagle's medium (DMEM), fetal bovine serum (FBS) and penicillin–streptomycin were purchased from Invitrogen. All solvents used were of high-performance liquid chromatography (HPLC) grade. The water used in this study was provided by a Milli-Q water purification system from Millipore. The antibodies PARP (CST, no. 9542), Cleaved-PARP (CST, no. 9541), active-caspase-3 (CST, no. 9664p), active-caspase-7 (CST, no. 9491), active-caspase-9 (CST, no. 9509s), Bad (CST, no. 9292), Bax (CST, 2772), Bcl-2 (CST, 2872), Bcl-XL (CST, 2762), general caspases inhibitor (z-VAD-fmk), caspase-9 inhibitor (z-LEHD-fmk) and caspase-3 inhibitor (z-DEVD-fmk) used in this study were all obtained from Cell Signaling Technology (Beverly, MA, USA).

Cell culture and drug treatments

U87 and U251 cells were purchased from American Type Culture Collection (ATCC, USA) and cultured in DMEM with fetal bovine serum (10 %), penicillin (100 U/ml) and streptomycin (50 U/ml) at 37 °C in a humidified incubator with 5 % CO_2 atmosphere. Cells (4×10^3 cells/well) seeded in a 96-well plate were exposed to caudatin (0, 25, 50, 100 μM) for 24, 48 and 72 h. The sensitive cell line to caudatin was employed for subsequent experiments.

MTT assay

Cell viability was detected by MTT assay. Briefly, U87 and U251 cells (4×10^3 cells/well) seeded in a 96-well plate were treated with caudatin (0, 25, 50, 100 μM) for 24, 48 and 72 h. After incubation, 20 μl MTT (5 mg/ml) solution/well was added and incubated for another 4 h. Then, the medium was aspirated, and 150 μl/well DMSO

was added to dissolve the formazan. Then, the 96-well plate was shaken on a mini shaker for 20 min. The absorbance at 570 nm reflects the cell growth condition was recorded by a microplate reader (Molecular Device, USA). Cell viability was expressed as percentage of control (as 100 %). The half maximal inhibitory concentration (IC_{50}) was used to evaluate the anticancer ability of caudatin.

Cell cycle distribution and detection of cell apoptosis

Flow cytometric analysis was used to analyze cell cycle distribution and cell apoptosis. Briefly, U251 cells seeded in cell culture dishes (6 cm) were treated with caudatin (0, 25, 50, 100 μM) for 72 h. After treatment, cells were trypsinized and harvested by centrifugation. Then, cells were stained with PI solution after fixation with 70 % ethanol at −20 °C overnight. Labelled cells were washed and analyzed with a flow cytometry. The sub-G1 peak (hypodiploid DNA contents) was used to quantify the apoptotic cell death.

Detection of ROS, superoxide and GSH content

U251 cells were seeded in 96-well plate and incubated with 10 μM DCFH-DA probe for 15 min at 37 °C. Then, cells were washed with PBS and treated with different concentrations of caudatin for 2 h. Then, the ROS level was monitored with microreader at excitation and emission wavelengths of 488 and 525 nm, respectively. The superoxide was detected by a mitochondria-targeted fluorogenic dye, MitoSOX (Beyotime). Briefly, U251 cells were seeded in 2-well plate and incubated with 10 μM MitoSOX probe for 15 min at 37 °C. Then, cells were washed with PBS and treated with different concentrations of caudatin for 2 h. The cells were then imaged with an inverted fluorescence microscope. The GSH content was determined by specific assay kits purchased from Beyotime Institute of Biotechnology and carried out according to the manufacturer's instructions. The data was expressed as percent of control (as 100 %). Cells were pretreated with GSH (ROS scavenger) for 2 h prior to the caudatin treatment to evaluate caudatin-induced cell growth inhibition and apoptosis.

Measurement of mitochondrial membrane potential (Δψm) and mitochondrial mass

U251 cells seeded in a tissue culture plate (2 cm) were incubated with 10 μg/ml JC-1 solution at 37 °C for 15 min. After incubation, cells were washed with PBS and treated with caudatin for 5, 15 and 30 min. At the different interval, the Δψm of the same area of cells were examined by a fluorescence microscope (Nikon Eclipse80i, ×200). The shift of fluorescence from red to green represents the loss of Δψm. The mitochondrial mass was detected by NAO probe. Briefly, cells seeded in 2-cm tissue culture plates were exposed to 25–100 μM caudatin for 72 h. After treatment, cells were incubated with 10 μM NAO and 10 μg/ml DAPI for 15 min. Then, cells were washed and observed by fluorescence microscope (Nikon Eclipse80i, ×200). The mitochondrial mass was analysed by Image-Pro Plus 6.0 (control as 100 %).

Western blotting

U251 cells were seeded in cell culture dishes (10 cm) and treated with caudatin (0, 25, 50, 100 μM) for 72 h. After treatment, the cells were washed with PBS, harvested and lysed with RIPA buffer. Total protein was extracted and quantified by BCA assay kit according to the manufacturer's instructions. The protein expression in U251 cells was detected by western blotting methods. Briefly, protein was boiled for 10 min and stored at −80 °C environments for subsequent test. Forty micrograms of total protein/lane was loaded and separated in 10 % SDS-PAGE. After electrophoresis, protein was transferred to polyvinylidene difluoride (PVDF) membranes. Then, the membrane was blocked with 5 % BSA for 2 h at room temperature, followed by incubation with primary antibodies (1:1000) overnight at 4 °C and secondary antibodies (1:2000) for 2 h at room temperature. Protein bands were detected by X-ray film using an enhanced chemiluminescence system (Nikon). The β-actin was employed as positive control band. The protein expressions were quantified by Quantity-One Software and the expression rate was labelled under the bands.

In vivo study

Briefly, about 1×10^7 U251 human glioma cells (in 100 μl serum-free medium) were subcutaneously

injected into the right oxter of male nude mice. After 8-day growth (tumour volume about 60 mm^3), the mice were treated with caudatin. Caudatin (0, 25 and 50 mg/kg) was injected from the caudal vein every other day from the first day until the 16th day (eight times). After experiments, tumours were harvested and measured with the following formula: volume $= 1 \times w^2/2$, with 1 being the maximal length and w being the width. Sections of tumours were used for western blotting and immunohistochemical (IHC) assay. The in vivo study was mainly conducted as in a previous report (Fan et al. 2014a, b). All animal experiments were approved by the Animal Experimentation Ethics Committee.

Statistical analysis

Statistical analysis was performed using the SPSS statistical package (SPSS 13.0 for Windows; SPSS, Inc., Chicago, IL USA). The difference between two groups was analyzed by a two-tailed Student's t test. The difference between three or more groups was analyzed by one-way analysis of variance multiple comparisons. Bars in figures with different characters (a, b, c or d) are statistically different at the $P < 0.05$ level, which were achieved by multiple comparison between three or more groups.

Results

Caudatin inhibits human glioma cells growth

Cell growth inhibition of caudatin against U251 and U87 cells was firstly assessed by MTT assay. As shown in Fig. 1a, b, caudatin treatment significantly decreased U251 and U87 cell viability in both a time- and dose-dependent manner. For instance, cells treated with caudatin (25, 50 and 100 μM) for 72 h significantly inhibited the U251 cell viability from 100 % (control) to 73.5, 51.3 and 28.2 %, respectively. The result suggested that caudatin could act as a potential cytostatic

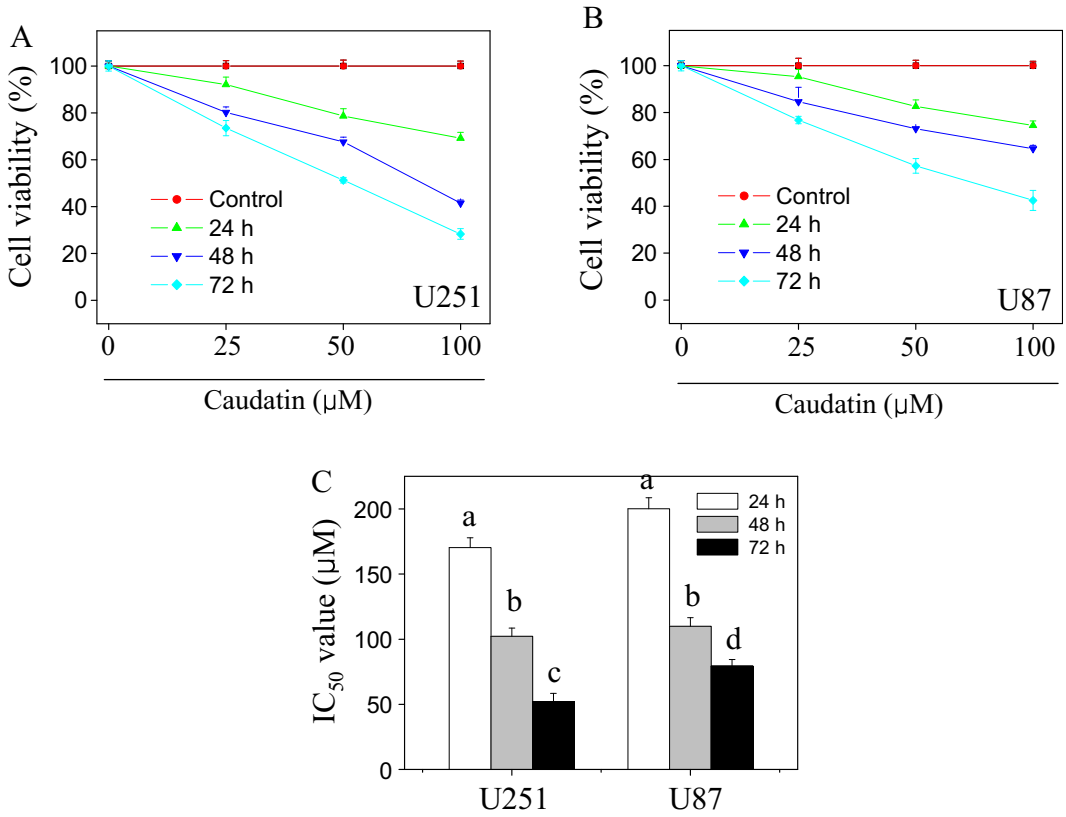

Fig. 1 Caudatin inhibits human glioma growth. Cytotoxicity of caudatin towards U251 (**a**) and U87 (**b**) cells. Cells seeded in 96-well plate (4000 cells/well) were treated with caudatin (0, 25, 50 or 100 μM) for 24, 48 and 72 h. Cell viability was detected by MTT assay. **c** The IC_{50} value of U251 and U87. All data were expressed as the mean ± SD of the three independent experiments. *Bars with different letters* indicate the statistical difference ($P < 0.05$)

agent in inhibiting human glioma cell growth. Moreover, the IC_{50} (half maximal inhibitory concentration) of caudatin at 24, 48 and 72 h towards U251 cells was 170.3, 102.2 and 52.1 μM, respectively (Fig. 1c), which showed more sensitivity to caudatin than that of U87 cells. Therefore, U251 cell line was employed for subsequent mechanism evaluation.

Caudatin induces glioma cell apoptosis

To elucidate the cell death mode, flow cytometric analysis was employed to detect caudatin-induced cell apoptosis. Apoptotic cells measured by flow cytometry usually emerge a Sub-G1 peak, which is generally used to quantify the cell apoptosis (Chen and Wong 2008). As shown in Fig. 2a, exposure of U251 cells to indicated concentrations of caudatin for 72 h resulted in significant cell apoptosis in a dose-dependent manner, as indicated by the increase of Sub-G1 peak. For instance, treatment with 50 and 100 μM caudatin caused 34.7 and 71.4 % apoptosis in U251 cells. Caudatin-induced apoptosis in human glioma cells was further confirmed in U87 cells, and the result indicated that induction of cell apoptosis was also the action model of caudatin against U87 cells (Figure S2). To further explore the apoptotic mechanism, PARP cleavage and caspase activation, two important apoptotic events, were investigated in caudatin-treated U251 cells by western blotting method. As shown in Fig. 2b, c, caudatin treatment significantly induced the PARP cleavage and the activation of caspase-3, caspase-7 and caspase-9, which further confirmed caudatin-induced apoptosis. The

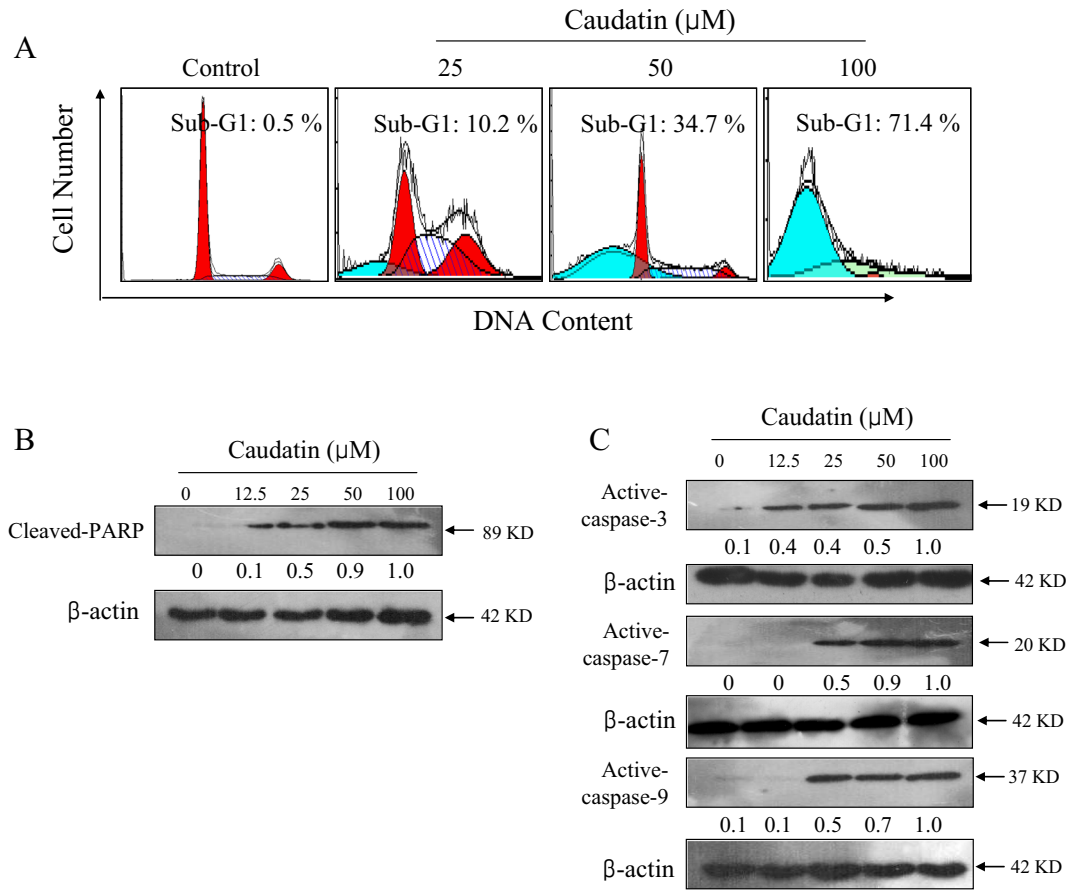

Fig. 2 Caudatin induces U251 cell apoptosis. **a** Flow cytometric analysis of caudatin-induced apoptosis in U251 cells. Cells after treatment with caudatin were stained with PI solution and detected by flow cytometry. The Sub-G1 peak was used to quantify the apoptotic cells. Caudatin induces U251 cell PARP cleavage (**b**) and caspase activation (**c**). Cells after treatment with caudatin were lysed and total protein (40 μg/lane) was loaded, and the protein expression was examined by western blotting method as presented in the "Materials and methods" section. The protein expressions were quantified by Quantity-One Software and the expression rate was labelled under the bands. All data and images were obtained from three independent experiments

activation of caspase-9 and caspase-7, two major initiators of mitochondria-mediated apoptotic pathway, suggests that caudatin inhibits human glioma cell growth mainly by induction of mitochondria-mediated apoptosis. To validate the contribution of death receptor-mediated extrinsic pathway, caspase-8 and DR5 expression were detected by western blotting method. The results indicated that caudatin treatment slightly activated caspase-8 and DR5, indicating that death receptor-mediated extrinsic pathway partly contributed to caudatin-induced U251 cell apoptosis.

Caudatin causes mitochondrial dysfunction

Mitochondria as the energy generator regulates both the extrinsic (death receptor-mediated) and intrinsic apoptotic (mitochondria-mediated) signals and plays key role in launching the apoptotic process (Marini et al. 2006).

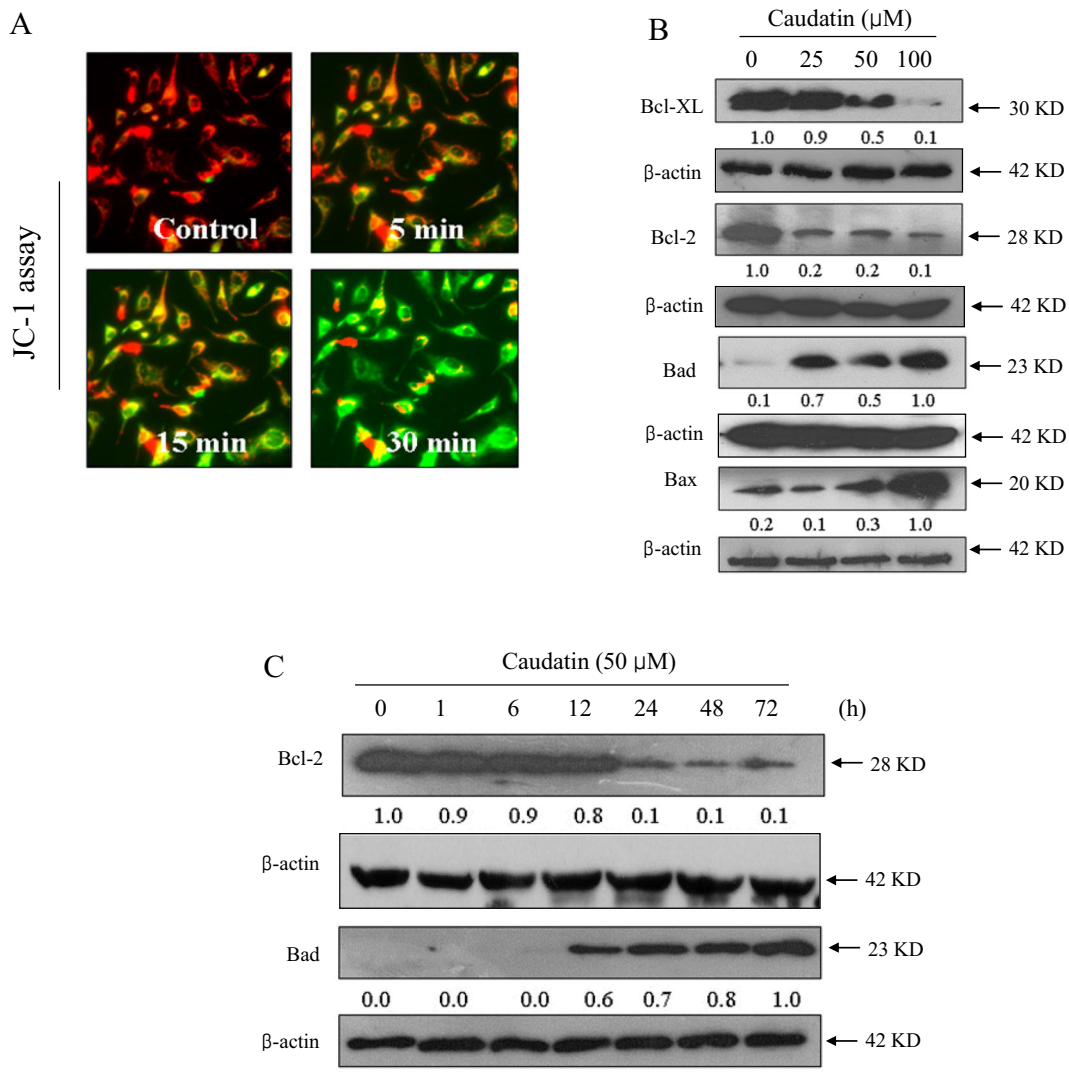

Fig. 3 Caudatin causes the mitochondrial dysfunction through dysregulation of Bcl-2 family. **a** Caudatin treatment resulted in the loss of mitochondrial membrane potential ($\Delta\psi m$). U251 cells seeded in a tissue culture plate (2 cm) were incubated with 10 μg/ml JC-1 solution at 37 °C for 15 min. After incubation, cells were washed with PBS and treated with caudatin for 5, 15 and 30 min. The Δψm of the same area of cells at different interval were imaged by a fluorescence microscope. The fluorescent shift from red to green indicates the depletion of ΔψmΔψm. **b** Caudatin affects Bcl-2 family expression. The protein expression was detected by Western blotting method. **c** Time-course effect of caudatin on Bcl-2 and Bad expression. The protein expressions were quantified by Quantity-One Software and the expression rate was labelled under the bands. All data and images were obtained from three independent experiments

Mitochondrial dysfunction will disturb the energy metabolism and lead to cell apoptosis. The loss of Δψm as an early apoptotic event contributes to the initiation of apoptotic cascades (Ryu et al. 2005). Therefore, we employed JC-1 probe to detect the loss of Δψm by fluorescence microscope. As shown in Fig. 3a, U251 cells treated with caudatin (50 μM) showed notable loss of Δψm in a time-dependent manner, as convinced by the enhanced green

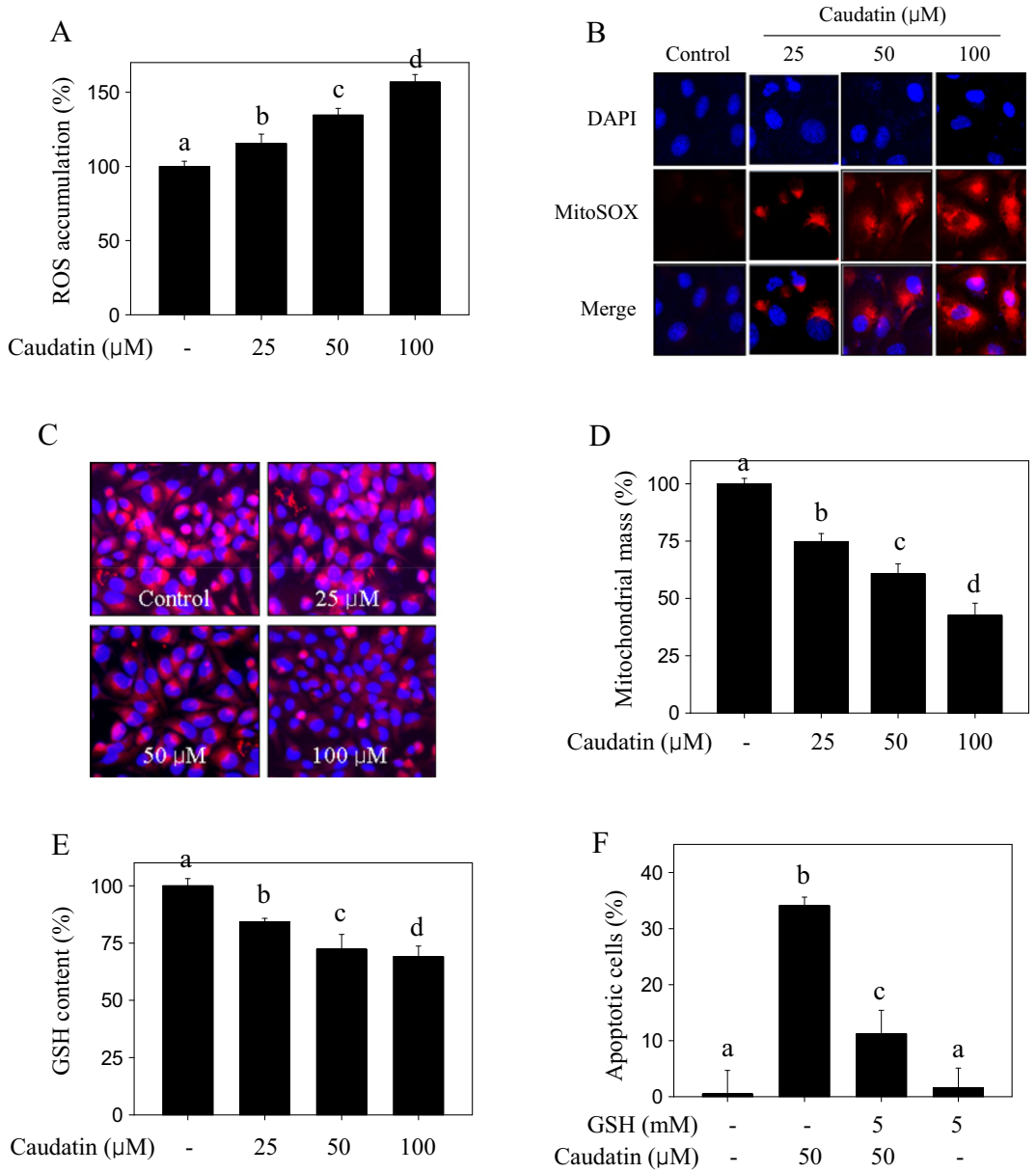

Fig. 4 Caudatin disturbs the intracellular redox homeostasis. **a** Caudatin induced ROS accumulation. **b** Caudatin caused superoxide production. The superoxide in live cells was detected by MitoSOX specific red dye which can target mitochondria superoxide (magnification, ×400). **c** Caudatin decreased the mitochondrial mass in U251 cells. Cells after treatment were stained by NAO and DAPI probes according to the description in section of methods. **d** Statistical analysis of mitochondrial mass by Image-Pro Plus 6.0. All images shown here are representative of three independent experiments with similar results. **e** Caudatin decreased the intracellular GSH content. The intracellular GSH content was measured by specific assay kits according to the manufacturer's instructions. **f** Inhibition of ROS attenuated caudatin-induced apoptosis. Cells were pretreated with glutathione (GSH) for 2 h before caudatin treatment. All data and images were obtained from three independent experiments. *Bars with different letters* indicate the statistical difference ($P < 0.05$)

fluorescence, followed by the decrease of red fluorescence. Furthermore, the mitochondrial mass was also examined by NAO probe. As shown in Fig. 4c, caudatin treatment dose-dependently decreased the mitochondrial mass, as proved by the decreased red fluorescence. The statistical analysis of mitochondrial mass further confirmed this conclusion (Fig. 4d). These results suggest that caudatin causes mitochondrial dysfunction.

Bcl-2 family members can affect Δψm and play important role in regulating cell apoptosis (Liu et al. 2014; Hollville et al. 2014; Kale et al. 2014). Hence, the Bcl-2 family was detected by western blotting. As shown in Fig. 3b, caudatin treatment dose-dependently upregulated the Bad and Bax expression, but downregulated the Bcl-2 and Bcl-XL expression. The time-course of Bcl-2 and Bad expression further confirmed that caudatin treatment disrupted the balance of Bcl-2 family member (Fig. 3c). Taken together, these results clearly revealed that caudatin caused mitochondrial dysfunction which correlated with an imbalance of Bcl-2 family members.

Caudatin disturbs the intracellular redox homeostasis

Based on the importance of the redox homeostasis, we examined the intracellular ROS generation, including the total ROS and superoxide anion. As shown in Fig. 4a, caudatin treatment significantly induced the total ROS accumulation with a dose-dependent manner. Moreover, the superoxide anion in live cells was detected by mitoSOX specific red dye which can target mitochondrial superoxide, and the result vividly indicated that caudatin dose-dependently induced superoxide anion production in live cells, as convinced by the enhanced red fluorescence (Fig. 4b). Additionally, caudatin treatment also decreased the glutathione content (GSH). However, GSH supplement effectively blocked caudatin-induced apoptosis in U251 cells, indicating the role of ROS in caudatin-induced apoptotic signal. These results all revealed that caudatin disturbed the intracellular redox homeostasis.

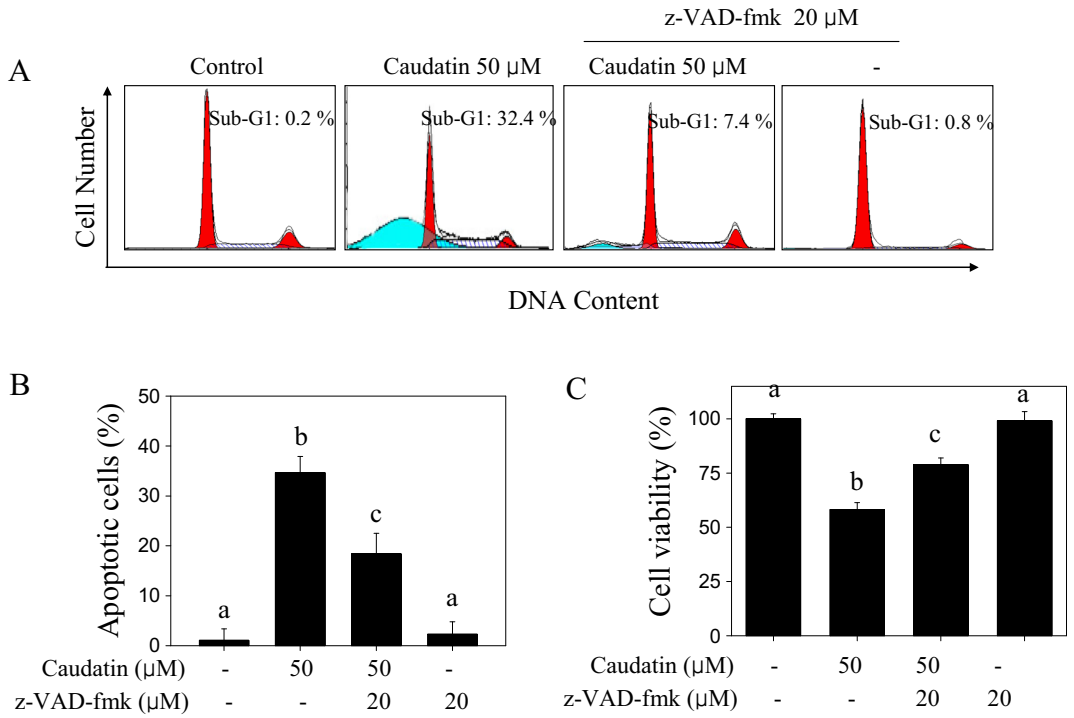

Fig. 5 Caudatin triggers caspase-dependent apoptosis in U251 cells. **a** z-VAD-fmk blocks caudatin-induced U251 cells apoptosis. Cells were pretreated with 20 μM z-VAD-fmk (a general caspase inhibitor) for 2 h prior to caudatin treatment. Cell apoptosis was analysed by flow cytometry analysis. **b** Statistical analysis of apoptotic cell death percentage. **c** z-VAD-fmk prevents caudatin-induced U251 cell killing. Cell viability was determined by MTT assay. All data were expressed as the mean ± SD of three independent experiments. *Bars with different characters* are statistically different at the $P < 0.05$ level. The protein expressions were quantified by Quantity-One Software and the expression rate was labelled under the bands. *Bars with different letters* indicate the statistical difference

Caudatin triggers caspase-dependent apoptosis in U251 cells

The caspase family plays a crucial role in initiating and modulating the apoptosis process. Based on the importance of caspase, z-VAD-fmk (a general caspases inhibitor) was employed to examine caudatin-induced apoptotic mechanism. Firstly, flow cytometric analysis revealed that z-VAD-fmk pretreatment effectively inhibited caudatin-induced apoptosis in U251 cells, as convinced by the weaken Sub-G1 peak (Fig. 5a). For instance, 50-μM caudatin treatment alone caused 32.4 % apoptosis. However, pretreatment with z-VAD-fmk effectively decreased the sub-G1 peak to 7.4 %. Moreover, inhibition of caspases subsequently large-scale elevated the cell viability and repressed the cell apoptosis in caudatin-treated cells, which indicated that caudatin induced cell growth inhibition and apoptosis in U251 cells in a caspase-dependent manner.

For further evaluation of caudatin-induced apoptosis, the effects of z-VAD-fmk (a general caspase inhibitor), z-LEHD-fmk (a caspase-9 inhibitor) and z-DEVD-fmk (a caspase-3 inhibitor) on PARP and caspase expression were also examined by western blotting. As shown in Fig. 6a, exposure of U251 cells to 50 μM caudatin alone markedly induced PARP cleavage and activation of caspase-3, caspase-7 and caspase-9. However, pretreatment with 20 μM z-VAD-fmk and z-LEHD-fmk dramatically suppressed caudatin-induced PARP cleavage (Fig. 6a). Moreover, addition of z-VAD-fmk and z-DEVD-fmk also suppressed caudatin-induced activation of caspases (Fig. 6b, c). Cells treated with z-VAD-fmk, z-LEHD-fmk or z-DEVD-fmk alone showed no significant changes in expression of PARP or caspases. Above all, these results all convinced that caudatin inhibits U251 cell growth by induction of caspase-dependent apoptosis.

Caudatin inhibits U251 tumour xenografts in vivo

To validate the in vivo effect and mechanism of caudatin against human glioma cell growth, the immunodeficient

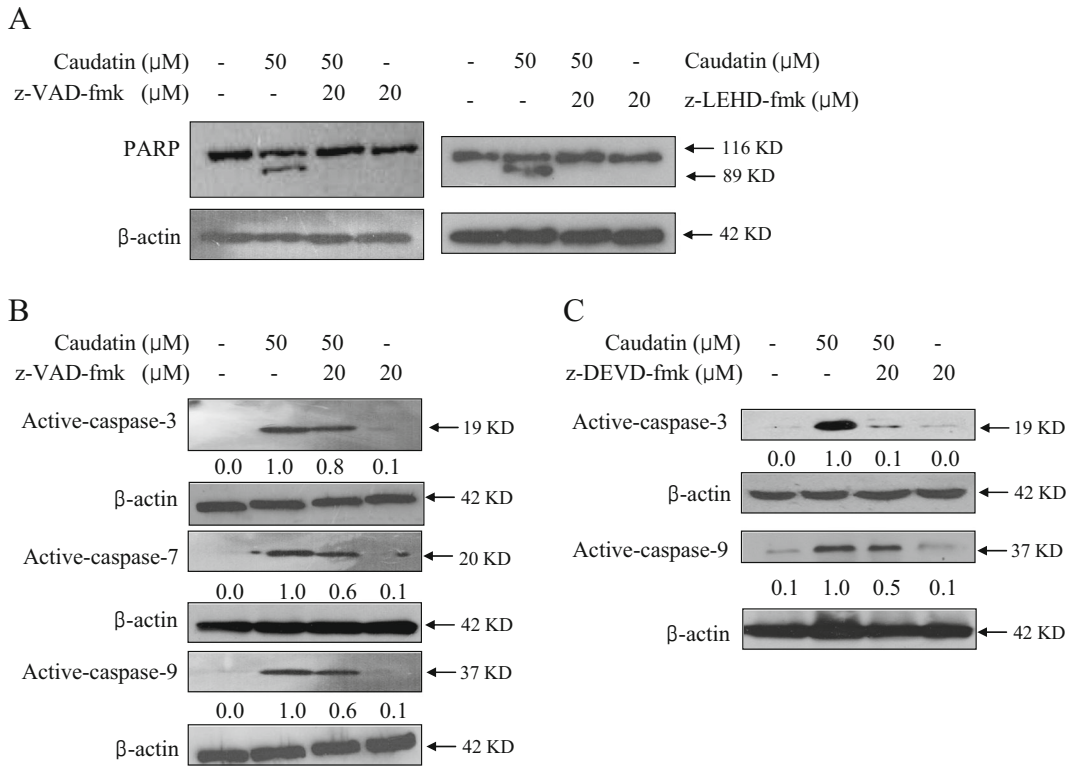

Fig. 6 Effect of z-VAD-fmk and z-LEHD-fmk on PARP and active-caspase expression in caudatin-treated U251 cells. **a** z-VAD-fmk and z-LEHD-fmk represses caudatin-induced PARP cleavage. **b** z-VAD-fmk alleviates caudatin-induced caspases activation. **c** z-DEVD-fmk inhibits caudatin-induced caspases activation. The protein expression of were detected by western blotting. All images were obtained from three independent experiments

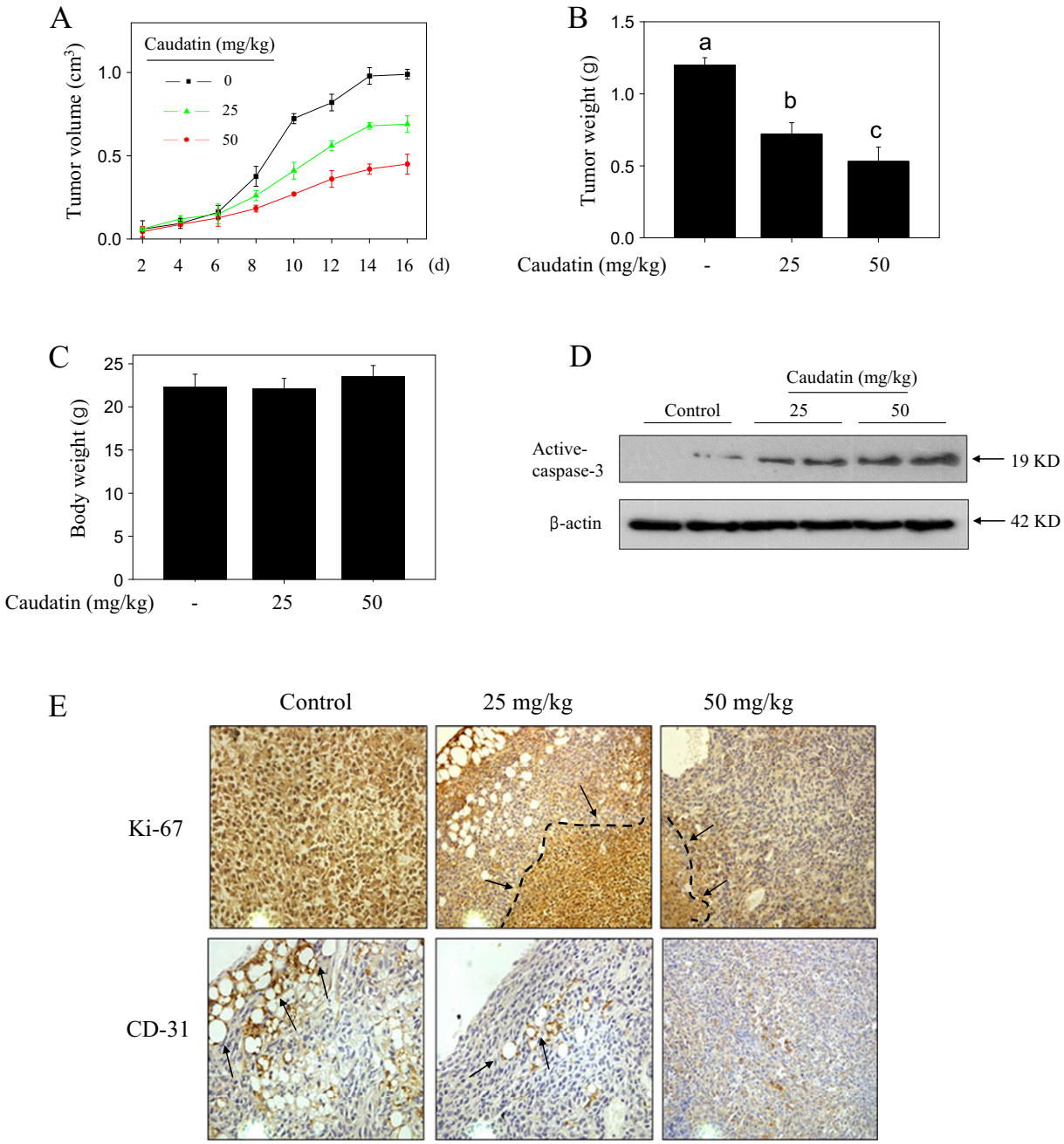

Fig. 7 Caudatin inhibits the growth of tumour xenografts in vivo. Caudatin treatment inhibits tumour volume (**a**) and tumour weight (**b**) of U251 human glioma xenografts in nude mice, but causes no affect on the mice body weight (**c**). **d** Caudatin treatment induces cell apoptosis in vivo. The active caspase-3 expression in vivo was detected by western blotting method. **e** Caudatin treatment suppresses the cell proliferation and angiogenesis in vivo. The Ki-67 and CD-31 expressions in vivo were examined by IHC method

nude mice bearing U251 tumour xenografts was employed. The results suggested that caudatin treatment in vivo significantly inhibited xenograft tumour growth, as convinced by the decrease of tumour volume (Fig. 7a) and tumour weight (Fig. 7b), but not affected body weight of mice (Fig. 7c). The mechanism studies in vivo revealed that caudatin treatment inhibited tumour xenografts by induction of cell apoptosis, as convinced by the activation of caspase-3 (Fig. 7d). Moreover, the cell proliferation and angiogenesis in vivo were also

evaluated by the IHC method, and the results indicate that caudatin treatment apparently inhibited cell proliferation (Ki67 staining) and angiogenesis (CD-31 staining) in vivo (Fig. 7e), which further validate its value in combating human glioma in vivo.

Discussion

Glioma with high infiltration and invasion capacity into adjacent tissues represents one of the most common malignant tumours of the nervous system. Thus, searching novel anticancer agents with high efficiency and low toxicity is emerging as the priority in clinical practice. Caudatin isolated from the root of *Cynanchum bungei decne* shows various pharmacological functions, including its antitumour activity. Our previous study has indicated that caudatin had the ability to inhibit human glioma cell growth in vitro, and induction of cell cycle arrest was accepted as the main anticancer mechanism after 48-h treatment (Fu et al. 2015). However, caudatin-induced apoptosis and the underlying mechanism remain elusive. Therefore, we reduced the cell density and prolonged the treatment time in the present study, and caudatin-induced apoptosis and mechanism were investigated in human glioma cells.

Apoptosis, a process of automatic killing, is tightly regulated by multiple gene and protein factors (Kang et al. 2006; Lu et al. 2015). Normal cell apoptosis can remove the useless, aging and some harmful cells to maintain the stability of homeostasis in case of cancers (Roos et al. 2007; Hsiao et al. 2009; Zhang et al. 2012; Lin et al. 2012). Thus, cancer cell apoptosis by antitumour drugs is the most important way in treating human tumours (Kang et al. 2006; Miyashita et al. 2006; Renaudo et al. 2004; Bose et al. 2010). However, drugs inhibit cancer cell growth by cell cycle arrest, apoptosis or combined model, which mainly depend on the cell types, cell concentration, drugs' properties, drug treatment time and dosage and so on. In our previous publication, U251 cells were seeded in a high density (10^5 cells/ml) and treated with caudatin for 48 h, and the results indicated that caudatin inhibited human glioma cell growth under thus condition mainly by triggering cell cycle arrest (Fu et al. 2015). However, in the present study, in order to exactly evaluate caudatin-induced apoptosis, the cells were seeded in a lower density (4×10^4 cells/ml) and the treatment time was prolonged to 72 h. As expected, U251 and U87 cells treated with caudatin for 72 h both showed significant cell apoptosis, as convinced by the increase of Sub-G1 peak, PARP cleavage, caspase activation and the mitochondria dysfunction. We speculated that cells with high density and short treatment time inevitably have stronger resistance against drug-induced cell apoptosis. Cells hence mainly initiated cell cycle arrest for DNA damage repair in our previous report (Fu et al. 2015). However, in the present study, the cells with low density and long treatment time inevitably mainly launched cell apoptosis to permanently remove the damaged cells. The similar conclusion was observed again recently in our recent publication (Wang et al 2016) and previous publication (Chen and Wong 2009).

Mitochondria integrate the extrinsic and intrinsic apoptotic signals and play an important role in launching mitochondria-mediated apoptosis (Lin et al. 2012; Ofengeim et al. 2012). Bcl-2 family including anti-apoptotic members (Bcl-2 and Bcl-XL) and proapoptotic members (Bax and Bad) is much involved in mitochondria-mediated apoptosis (Anilkumar and Prehn 2014; Bauer et al. 2015). The imbalance of Bcl-2 family expression and the loss of $\Delta\psi m$ both contribute to mitochondria-mediated apoptosis pathway (Sochalska et al. 2015; Kale et al. 2014). Caspases, a family of cysteine proteases, are synthesized as inactive proenzymes which are processed to active form in cells undergoing apoptosis (Bate et al. 2010). Caspase-3 is considered to be the most important executioner of apoptosis and caspase-7 and caspase-9 were accepted as the main regulators in mitochondria-mediated apoptosis (Droga-Mazovec et al. 2008; White et al. 2008; Xu et al. 2009). In this study, U251 cells treated with caudatin showed obvious loss of $\Delta\psi m$ through dysregulation of Bcl-2 family. Activation of caspase-3, caspase-7 and caspase-9 in caudatin-treated cells were all observed, which suggested that caudatin induced mitochondria-mediated apoptosis. Addition of several caspase inhibitors distinctly prevented caudatin-induced apoptosis, indicating the caspase-dependent apoptosis in caudatin-treated cells.

ROS, including hydrogen peroxide, hydroxyl radical and superoxide anion, all have key roles in induction of cancer cell apoptosis (Chen and Wong 2008). The balance of the anti-antioxidant and pro-antioxidant system keeps the intracellular level of ROS. Therefore, induction of cell apoptosis by promoting ROS accumulation represents an important mechanism to combat human cancers. In the present study, ROS generation was

observed as early as in 15 min in caudatin-treated cells, confirming the important role of ROS as an early event in apoptotic signal. Fei et al. previously reported that caudatin could induce caspase-dependent apoptosis in HepG2 human hepatocarcinoma with involvement of Bcl-2 family change and activation of ERK and JNK (Fei et al. 2012), but the role of reactive oxygen species (ROS) in caudatin-induced apoptosis in HepG2 cells was not investigated. We previously reported that caudatin-induced apoptosis involved AKT inactivation (Fu et al. 2015). Even though the role of MAPKs and AKT pathways in caudatin-induced apoptosis were not evaluated in the present study, we speculated that MAPKs and AKT pathways may both contribute to caudatin-induced apoptosis. Because our previous many publications revealed that ROS as an upstream mediator could play key role in regulating cell cycle arrest and apoptosis and regulating MAKPs and AKT pathways (Wang et al. 2015a, b; Fu et al. 2016; Fan et al. 2014a, b; Fan et al. 2013).

In conclusion, caudatin could act as an effective cytostatic agent in inhibiting human glioma cell growth through triggering mitochondria-mediated apoptosis. Mechanistically, caudatin lunches caspase-dependent apoptosis with involvement of mitochondrial dysfunction and ROS generation. Importantly, caudatin showed novel anti-tumor effect against U251 tumour xenografts in vivo through induction of cell apoptosis involving the inhibition of cell proliferation and angiogenesis, which validated the therapeutic potential of caudatin in hunting human glioma.

Acknowledgments The study was supported by the National Natural Science Foundation of China No. 81471212 to B.-L. Sun and 81501106 to C.-D. Fan. The Excellent Young and Middle-Aged Scientists Reward Foundation of Shandong No. BS2011YY058 to H.-L Gao.

Compliance with ethical standards

Conflict of interest The authors declare that they have no conflict of interest.

References

Adair JE, Johnston SK, Mrugala MM, Beard BC, Guyman LA, Baldock AL, et al. Gene therapy enhances chemotherapy tolerance and efficacy in glioblastoma patients. J Clin Invest. 2014;124:4082–92.

Anilkumar U, Prehn JH. Anti-apoptotic BCL-2 family proteins in acute neural injury. Front Cell Neurosci. 2014;8:281.

Bate C, Tayebi M, Williams A. A glycosylphosphatidylinositol analogue reduced prion-derived peptide mediated activation of cytoplasmic phospholipase A2, synapse degeneration and neuronal death. Neuropharmacology. 2010;59:93–9.

Bauer C, Hees C, Sterzik A, Bauernfeind F, Mak'Anyengo R, Duewell P, et al. Proapoptotic and antiapoptotic proteins of the Bcl-2 family regulate sensitivity of pancreatic cancer cells toward gemcitabine and T-cell-mediated cytotoxicity. J Immunother. 2015;38:116–26.

Bose PS, Naspinski J, Kartha G, Bennett PS, Wang CJ, Haynes JI, et al. Development of a high-throughput rubella virus infectivity assay based on viral activation of caspases. J Virol Methods. 2010;167:199–204.

Chen T, Wong YS. Selenocystine induces S-phase arrest and apoptosis in human breast adenocarcinoma MCF-7 cells by modulating ERK and Akt phosphorylation. J Agric Food Chem. 2008;56:10574–81.

Chen T, Wong YS. Selenocystine induces reactive oxygen species-mediated apoptosis in human cancer cells. Biomed Pharmacother. 2009;63:105–13.

Demuth T, Rennert JL, Hoelzinger DB, Reavie LB, Nakada M, Beaudry C, et al. Glioma cells on the run-the migratory transcriptome of 10 human glioma cell lines. BMC Genomics. 2008;9:54.

Droga-Mazovec G, Bojic L, Petelin A, Ivanova S, Romih R, Repnik U, et al. Cysteine cathepsins trigger caspase-dependent cell death through cleavage of bid and antiapoptotic Bcl-2 homologues. J Biol Chem. 2008;283:19140–50.

Fan CD, Chen JJ, Wang Y, Wong YS, Zhang YB, Zheng WJ, et al. Selenocystine potentiates cancer cell apoptosis induced by 5-fluorouracil by triggering ROS-mediated DNA damage and inactivation of ERK pathway. Free Radic Biol Med. 2013;65:305–16.

Fan CD, Zheng WJ, Fu XY, Li XL, Wong YS, Chen TF. Strategy to enhance the therapeutic effect of doxorubicin in human hepatocellular carcinoma by selenocystine, a synergistic agent that regulates the ROS-mediated signaling. Oncotarget. 2014a;5:2853–63.

Fan CD, Zheng WJ, Fu XY, Li XL, Wong YS, Chen TF. Enhancement of auranofin-induced lung cancer cell apoptosis by selenocystine, a natural inhibitor of TrxR1 in vitro and in vivo. Cell Death Dis. 2014b;5:e1191.

Fei HR, Chen HL, Xiao T, Chen G, Wang FZ. Caudatin induces cell cycle arrest and caspase-dependent apoptosis in HepG2 cell. Mol Biol Rep. 2012;39:131–8.

Fu XY, Zhang S, Wang K, Yang MF, Fan CD, Sun BL. Caudatin inhibits human glioma cells growth through triggering DNA damage-mediated cell cycle arrest. Cell Mol Neurobiol. 2015;35:953–9.

Fu XY, Yang MF, Cao MZ, Li DW, Yang XY, Sun JY, et al. Strategy to suppress oxidative damage-induced neurotoxicity in PC12 cells by curcumin, the role of ROS-mediated DNA damage and MAPKs and AKT pathways. Mol Neurobiol. 2016;53:369–78.

Hollville E, Carroll RG, Cullen SP, Martin SJ. Bcl-2 family proteins participate in mitochondrial quality control by regulating Parkin/PINK1-dependent mitophagy. Mol Cell. 2014;55:451–66.

Hsiao JR, Leu SF, Huang BM. Apoptotic mechanism of paclitaxel-induced cell death in human head and neck tumour cell lines. J Oral Pathol Med. 2009;38:188–97.

Kale J, Chi X, Leber B, Andrews D. Examining the molecular mechanism of bcl-2 family proteins at membranes by fluorescence spectroscopy. Methods Enzymol. 2014;544:1–23.

Kang SK, Cha SH, Jeon HG. Curcumin-induced histone hypoacetylation enhances caspase-3-dependent glioma cell death and neurogenesis of neural progenitor cells. Stem Cells Dev. 2006;15:165–74.

Li X, Zhang M, Xiang C, Qin Y, He J, Li BC, et al. C21 steroids from roots of Cynanchum otophyllum. Zhongguo Zhong Yao Za Zhi. 2014;39:1450–6.

Lin CJ, Lee CC, Shih YL, Lin CH, Wang SH, Chen TH, et al. Inhibition of mitochondria- and endoplasmic reticulum stress-mediated autophagy augments temozolomide-induced apoptosis in glioma cells. PLoS ONE. 2012;7:e38706.

Liu D, Yi B, Liao Z, Tang L, Yin D, Zeng S, et al. 14-3-3gamma protein attenuates lipopolysaccharide-induced cardiomyocytes injury through the Bcl-2 family/mitochondria pathway. Int Immunopharmacol. 2014;21:509–15.

Lu DF, Wang YS, Li C, Wei GJ, Chen R, Dong DM, et al. Actinomycin D inhibits cell proliferations and promotes apoptosis in osteosarcoma cells. Int J Clin Exp Med. 2015;8:1904–11.

Luo Y, Sun Z, Li Y, Liu L, Cai X, Li Z. Caudatin inhibits human hepatoma cell growth and metastasis through modulation of the Wnt/beta-catenin pathway. Oncol Rep. 2013;30:2923–8.

Lv W, Zhang A, Xu S, Zhang H. Effects of general glycosides in Cynanchum auriculatum of Jiangsu province on liver fibrosis of rats. Zhongguo Zhong Yao Za Zhi. 2009;34:2508–11.

Ma XX, Wang D, Zhang YJ, Yang CR. Identification of new qingyangshengenin and caudatin glycosides from the roots of Cynanchum otophyllum. Steroids. 2011;76:1003–9.

Marini P, Denzinger S, Schiller D, Kauder S, Welz S, Humphreys R, et al. Combined treatment of colorectal tumours with agonistic TRAIL receptor antibodies HGS-ETR1 and HGS-ETR2 and radiotherapy: enhanced effects in vitro and dose-dependent growth delay in vivo. Oncogene. 2006;25:5145–54.

Miyashita K, Shiraki K, Fuke H, Inoue T, Yamanaka Y, Yamaguchi Y, et al. The cyclin-dependent kinase inhibitor flavopiridol sensitizes human hepatocellular carcinoma cells to TRAIL-induced apoptosis. Int J Mol Med. 2006;18:249–56.

Ofengeim D, Chen YB, Miyawaki T, Li H, Sacchetti S, Flannery RJ, et al. N-terminally cleaved Bcl-xL mediates ischemia-induced neuronal death. Nat Neurosci. 2012;15:574–80.

Peng Y, Ding Y. Pharmacokinetics and tissue distribution study of caudatin in normal and diethylnitrosamine-induced hepatocellular carcinoma model rats. Molecules. 2015;20:4225–37.

Peng Y, Li Y, Wang D, Liu X, Zhang J, Qian S, et al. Determination of caudatin-2,6-dideoxy-3-O-methy-beta-d-cymaropyranoside in rat plasma using liquid chromatography-tandem mass spectrometry. Biomed Chromatogr. 2008;22:575–80.

Renaudo A, Watry V, Chassot AA, Ponzio G, Ehrenfeld J, Soriani O. Inhibition of tumour cell proliferation by sigma ligands is associated with K+ Channel inhibition and p27kip1 accumulation. J Pharmacol Exp Ther. 2004;311:1105–14.

Roos WP, Batista LF, Naumann SC, Wick W, Weller M, Menck CF, et al. Apoptosis in malignant glioma cells triggered by the temozolomide-induced DNA lesion O6-methylguanine. Oncogene. 2007;26:186–97.

Ryu HY, Emberley JK, Schlezinger JJ, Allan LL, Na S, Sherr DH. Environmental chemical-induced bone marrow B cell apoptosis: death receptor-independent activation of a caspase-3 to caspase-8 pathway. Mol Pharmacol. 2005;68:1087–96.

Sochalska M, Tuzlak S, Egle A, Villunger A. Lessons from gain- and loss-of-function models of pro-survival Bcl2 family proteins: implications for targeted therapy. FEBS J. 2015;282:834–9.

Teschke R, Eickhoff A. Herbal hepatotoxicity in traditional and modern medicine: actual key issues and new encouraging steps. Front Pharmacol. 2015;6:72.

Tseng MY, Tseng JH. Survival analysis for adult glioma in England and Wales. J Formos Med Assoc. 2005;104:341–8.

Wang YQ, Yang B, Zhang RS, Wei EQ. Inhibitive effect of C-21 steroidal glycosides of Cynanchum auriculatum on rat glioma cells in vitro. Zhejiang Da Xue Xue Bao Yi Xue Ban. 2011;40:402–7.

Wang YQ, Zhang SJ, Lu H, Yang B, Ye LF, Zhang RS. A C21-steroidal glycoside isolated from the roots of Cynanchum auriculatum induces cell cycle arrest and apoptosis in human gastric cancer SGC-7901 cells. Evid Based Complement Alternat Med. 2013. doi:10.1155/2013/180839.

Wang K, Fu XY, Fu XT, Hou YJ, Fang J, Zhang S, et al. DSePA antagonizes high glucose-induced neurotoxicity: evidences for DNA damage-mediated p53 phosphorylation and MAPKs and AKT pathways. Mol Neurobiol. 2015a. doi:10.1007/s12035-015-9373-1.

Wang Q, Wang Z, Chu L, Li X, Kan P, Xin X, et al. Dendritic cell-derived interleukin-15 is crucial for therapeutic cancer vaccine potenc. PLoS ONE. 2015b;10:e0125473.

Wang K, Fu XT, Li Y, Hou YJ, Yang MF, Sun JY, et al. Induction of S-phase arrest in human glioma cells by selenocystine, a natural selenium-containing agent via triggering reactive oxygen species-mediated DNA damage and modulating MAPKs and AKT pathways. Neurochem Res. 2016. doi:10.1007/s11064-016-1854-8.

White MK, Amini S, Khalili K, Kogan M, Donaldson K, Darbinian N. Development of a bidirectional caspase-3 expression system for the induction of apoptosis. Cancer Biol Ther. 2008;7:945–54.

Xu X, Liu Y, Wang L, He J, Zhang H, Chen X, et al. Gambogic acid induces apoptosis by regulating the expression of Bax and Bcl-2 and enhancing caspase-3 activity in human malignant melanoma A375 cells. Int J Dermatol. 2009;48:186–92.

Zhang R, Liu Y, Wang Y, Ye Y, Li X. Cytotoxic and apoptosis-inducing properties of auriculoside A in tumour cells. Chem Biodivers. 2007;4:887–92.

Zhang H, Zhang YW, Chen Y, Huang X, Zhou F, Wang W, et al. Apoptosin is a novel pro-apoptotic protein and mediates cell death in neurodegeneration. J Neurosci. 2012;32:15565–76.

Zhang Y, Tian S, Liu Z, Zhang J, Zhang M, Bosenberg MW, et al. The effects and molecular mechanisms of MiR-106a in multidrug resistance reversal in human glioma U87/DDP and U251/G cell lines. Oncoimmunology. 2014;3:e959321.